Thermionic and Surface Properties of Tungsten Crystals*

GEORGE F. SMITH†
California Institute of Technology, Pasadena, California
(Received November 9, 1953)

A plateau-like surface structure was found on single crystals grown in tungsten wire. Plateaus were observed on the surface normal to the (110), (112), and (001) directions. A "shingle" structure was observed superimposed upon the plateaus. A wire subjected to only mild heat treatment showed both types of structure, indicating that evaporation cannot be the only mechanism involved. All wires were heated by ac exclusively to avoid the "dc etch."

New values of the thermionic constants for different crystal directions were measured on a crystal having a minimum of shingling. Measurements were made in the tube previously used by Nichols, modified to eliminate an anomalous effect. The modification did not appreciably alter the emission constants for the (111), (112), (116), and (001) directions, which constants are in reasonable agreement with Nichols' values. A second anomalous effect contributed to currents measured in the low emission (110) direction, rendering normally obtained (110) values erroneous (including those of Nichols). Although the true (110) constants could not be obtained, an upper limit for the emission is characterized by $\varphi^{**}=4.72$, $A^{**}=9.7$ and two estimates of about 5.3 v are deduced for φ^{**}. There was no evidence in general for patchiness of the single crystal surfaces investigated; however, the usual tests cannot conclusively deny the existence of patchiness.

I. INTRODUCTION

THE technique of producing crystals of centimeter length in tungsten wire is well known. As a result of about 1 percent of "dope" consisting of Na_2O, K_2O, $CaCl_2$, Al_2O_3, and SiO_2 added before the sintering process,[1] the "nonsag" type of tungsten wire recrystallizes into crystals occupying the entire cross section of the wire. Robinson[2] has shown that under a favorable vacuum heat treatment schedule one can produce crystals several centimeters long in prewar nonsag tungsten wire. Chemical analyses of doped tungsten wire after the usual heat treatment associated with thermionic emission measurements show about the same very small relative impurity content as in undoped wire.[3] This fact along with thermionic emission stability through all temperature cycles after sufficient heat treatment, gives assurance that emission studies of doped wire are actually characteristic of pure tungsten.[3] As a result of the working given the wire during the drawing process, the crystals grown in doped wire are normally oriented with a face diagonal very nearly parallel to the wire axis. This orientation is particularly favorable to emission studies since, if the wire is smooth and round, the placing of the face diagonal along the wire axis causes directions emerging normal to the surface to include all directions with Miller indices of the form (*hhk*). Martin's work[4] with thermionic emission from a single crystal sphere of tungsten showed that the directions of principal interest, namely the maxima and minima of emission, are all of the form (*hhk*).[5]

Two kinds of surface structure have been observed on single crystals of tungsten heated in vacuum: (a) a so-called "dc etch," and (b) a "shingle" structure. The former effect was first reported by Johnson,[6] and has been studied by Schmidt[7] and by D. Langmuir.[8] It consists of a step-like structure found on wires subjected to prolonged heating with direct current; it also occurs near the supports of a wire heated with alternating current, where strong thermal gradients exist. The shingle structure was reported by Nichols[9] and was observed in the (110) crystal direction. Both structure effects were to be found on the crystal from which Nichols[9] obtained his emission constants as a function of crystallographic direction. Moreover, prior to the present investigation it has appeared plausible to explain the emission data for the (110) direction as being characteristic of a patch surface,[9,10] contributory evidence of the patchy nature deriving from the existence of the shingle structure on that surface. The principal objective of this research was to make thermionic measurements from a crystal (a) free from the dc etch and (b) with minimized shingle structure. Freedom from dc etch could readily be achieved by using only ac for filament heating. Indeed, Johnson[6] has reported that helical tungsten wires heated by ac in vacuum develop surfaces which appear to be free from any structure visible under a light microscope,

* This work was done with a facility created with the aid of a Research Corporation grant and was supported in part by the U. S. Office of Naval Research. It has been reported in greater detail in Final Report N6-onr-24433, June, 1952 (unpublished). Part of the work was done in partial fulfillment of the requirements for the Ph.D. degree at the California Institute of Technology.

† Now at Hughes Research and Development Laboratories, Culver City, California.

[1] C. J. Smithells, *Tungsten* (D. Van Nostrand Company, Inc., New York, 1936), second edition.

[2] C. S. Robinson, J. Appl. Phys. **13**, 647 (1942).

[3] M. H. Nichols, Phys. Rev. **78**, 158 (1950).

[4] S. T. Martin, Phys. Rev. **56**, 947 (1939).

[5] J. A. Becker, in private communication, has indicated that his field emission studies show that there may be a small field emission minimum in the vicinity of the (210) direction.

[6] R. P. Johnson, Phys. Rev. **54**, 459 (1938).

[7] R. W. Schmidt, Z. Physik **120**, 69 (1943).

[8] D. B. Langmuir, Phys. Rev. **89**, 911 (1953); **91**, 447 (1953).

[9] M. H. Nichols, Phys. Rev. **57**, 297 (1940).

[10] Conyers Herring and M. H. Nichols, Revs. Modern Phys. **21**, 185 (1949).

even after heating sufficient to evaporate away 17 percent of the wire. The shingle structure, however, has been found to occur on wires heated only with ac. Nevertheless, it was believed that this type of structure could be eliminated or at least greatly reduced by a careful examination and selection of the crystal to be used.

II. GROWTH AND SURFACE STRUCTURE OF SINGLE CRYSTALS OF TUNGSTEN

With this purpose in mind, a program of single-crystal production was instituted. Wires to be recrystallized were first polished[11] to remove die-marks and to produce a uniform circular cross section. The recrystallization process itself was carried out in what is commonly called an electron projection tube[12,9] after the method of Robinson.[2]

Six 14-in. lengths of 0.005-in. tungsten wire were recrystallized. Of the six, four were of G.E. No. 218 wire, dated 1939, each of which produced crystals several centimeters in length. The remaining two were of Callite No. 200*H*, dated 1940, neither of which produced crystals of more than millimeter length. One G.E. wire was recrystallized at 1980°K, producing a single, but relatively imperfect, crystal filling the 14-in. wire. The 2100°K runs each produced several crystals averaging three or four centimeters in length. In each case the orientation, length, and degree of perfection of single crystals produced were carefully noted from the emission pattern as observed in the projection tube. Cathetometer measurements were made to fix the position of each crystal section that showed an emission pattern free from flaws. Then the wire was removed from the projection tube, and each selected section was examined for structure visible under a light microscope of 100× magnification.

In each case it was possible to resolve shingle structure associated with the (110) direction, even in the case of wires subjected to only mild heat treatment. The 1980°K wire, given a total heat treatment of 22 hr at 1980°K plus 20 min at 2280°K, should have suffered an average diameter reduction of about 3×10^{-8} cm.[13] On this wire not only was the shingle structure observed on the two surfaces normal to (110) directions, but the shingles were superimposed upon what appeared to be a plateau, or flat surface, on the crystal. Even where the shingling was particularly faint, one could make out the plateau edges, separated by a few degrees of azimuth. Before prolonged heat treatment all recrystallized wires showed both these effects, as well as grain boundaries and occasional surface crystal "lakes."

The shingle structure observed in recrystallized wires before prolonged heat treatment varied both in form and visibility. The shingling is possibly a result of the failure of the crystal face diagonal to be aligned *precisely* along the wire axis. The orientation of the apexes of the shingles then indicates the direction of "dip" of the true crystal planes with respect to the wire surface. If a true cylinder were cut from a perfect

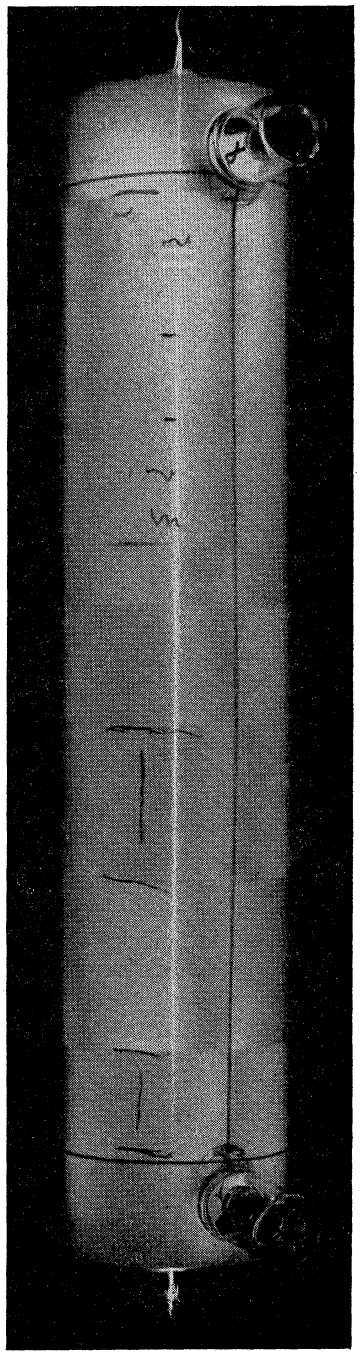

FIG. 1. Projection tube pattern of wire containing single crystal section used for quantitative thermionic measurements. The white marks set off the single crystal section; the dark marks are crayon lines on the tube for identification purposes.

[11] Johnson, White, and Nelson, Rev. Sci. Instr. **9**, 253 (1938).
[12] R. P. Johnson and W. Schockley, Phys. Rev. **49**, 436 (1936).
[13] H. A. Jones and I. Langmuir, Gen. Elec. Rev. **30**, 310; 354, 408 (1927).

crystal, one would expect to find opposite directions of dip and opposite orientation of shingle apexes on the opposite (110) surfaces. This was usually but not always found to be the case for the crystals examined. The few instances noted with the same apex orientation on both sides of the wire could be due to the presence of an undetected longitudinal grain boundary between the two sides of the wire; variation in wire diameter along the length of the crystal could also produce this effect. Longitudinal grain boundaries are common in in G.E. No. 218 wire, and would be difficult to observe on a wire given only mild heat treatment, especially if the orientations of the two crystals were not appreciably different; no examination of this phenomenon was made after prolonged heat treatment. In a few cases a (110) surface was found with a shingle-free region having oppositely oriented shingles at either end. A slight bend in the wire before recrystallization could produce this effect; Johnson[6] has reported that a single crystal grown in a tungsten helix maintains a fixed orientation in space as though the helix were carved out of a large crystal. In some isolated cases surfaces were found with little or no shingling in evidence over several millimeters along the axis of the wire. Both in obtaining a shingle-free (110) surface and in having precise (*hhk*) directions exhibited normal to the wire axis, such a section would show promise for quantitative thermionic measurements. At this point one of the four G.E. No. 218 wires was selected for further investigation. The recrystallization schedule of the wire is given in Table I, A; the projection tube pattern after recrystallization is shown in Fig. 1.

TABLE I. History of single crystal wire. Temperatures below 2100°K during taking of thermionic data are not listed.

Heat treatment	Subsequent observation
A. 2100°K, 15.5 hr; 2410°K, 10 min; 2610°K, 15.5 min; 2820°K, 0.5 min.	Plateaus in (110) directions, shingling.
B. 2610°K, 240 min; 2720°K, 30 min; 2820°K, 10 min; 2915°K, 2 min.	Little change in structure. Repolish.
C. 2760°K, 340 min; 2990°K, 10 min.	Similar structure restored.
D. 2700°K, 165 min; 2750°K, 51 min; 2830°K, 5 min.	Discover (001), (112) plateaus optically.
E. 2575°K, 32 min; 2775°K, 34 min.	Pre-end-guard thermionic data.
F. 2785°K, 38.5 min.	Final thermionic data.
G. 3030°K, 1 min; 2800°K, 5 sec; 1230°K, 92 hours.	Photograph plateaus, see Fig. 2.

To determine the effect of moderate heat treatment upon the size and shape of surface structure, the wire was subjected to the temperature schedule of Table I, B. Although this treatment left the surface in general almost entirely smooth and free from markings, the size and appearance of the plateaus and shingle structure were not materially altered. The recrystallized wire was then repolished (the diameter was reduced 1 percent) in order to determine whether the structure had been produced during recrystallization, not to return if once removed. After the relatively severe heat treatment of Table I, C (sufficient to evaporate about 2 percent of the diameter)[14] the plateau and shingle structure were observed to be restored to essentially the same condition as observed before repolishing. From the wire in this condition a single crystal section was selected for the quantitative thermionic measurements. The section chosen showed a minimum of shingling and lake structure together with a flawless qualitative emission pattern. This section is marked on Fig. 1. The further heat treatment listed in Table I was dictated by outgassing procedures. Very faint plateaus were also discovered optically in the (001) and (112) directions after a preliminary run in the thermionic measuring tube. At this time the wire had suffered less than 0.5 percent additional diameter reduction by evaporation due to the temperature schedule of Table I, D, making the total reduction about 2.5 percent from its value at the conclusion of repolishing.

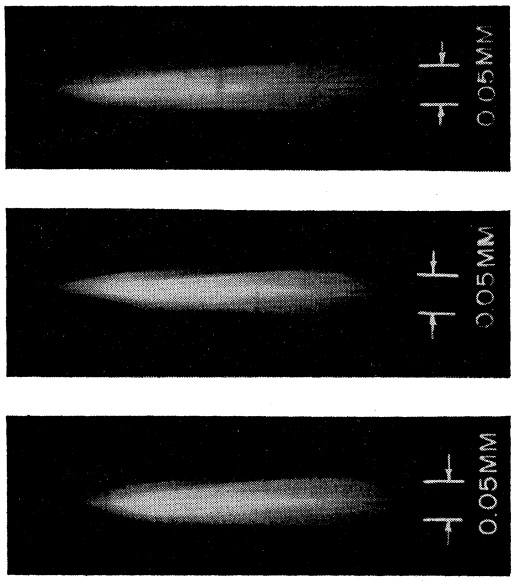

FIG. 2. Photomicrographs of single crystal showing plateau structure. (a) 180° (110) plateau; (b) 235° (112) plateau; (c) 90° (001) plateau.

At the conclusion of the final thermionic emission measurements (see Sec. V), subsequent to the heat treatment of Table I, EFG, the photomicrographs of Fig. 2 were taken of the surface structure on the chosen crystal section. Illumination at grazing incidence, obtained by adjusting the direct-dark field slide of the Zeiss Epi condenser microscope midway between the two usual positions, was found necessary to provide sufficient contrast to make out the smaller structure at all. The dimensions marked on the photographs and plateau widths listed in Table II were obtained by photographing an Eastman stage calibrated scale; the

[14] As measured by micrometer. From the Jones-Langmuir tables, reference 13, one computes a reduction three times as large. In general the evaporation computed by the Jones-Langmuir tables was greater than that observed by diameter measurements.

TABLE II. Plateau widths after heat treatment of Table I.

Direction of plateau	Width from photomicrograph	Width from emission plot	Orientation of shingling
0° (110)	11°	...	Left, faint
180° (110)	11°	Invalid (see Sec. IV)	Right, faint
55° (112)	7°	6.8°	None resolved
125° (112)	7°	6.3°	Right, very faint
235° (112)	7°	6.3°	None resolved
90° (001)	7°	7.8°	Right, faint

error in these measurements is probably less than 20 percent. The photomicrograph of the 90° (001) surface shows, in addition to the plateau, a very faint periodic diagonal scoring which has the pitch of the polishing machine screw. Although the average wire diameter at this point had been reduced about 3.6 percent by evaporation from the value after repolishing, it appears that faint markings in the vicinity of the (001) surface survived the heat treatment.

Additional evidence of the existence of (110), (112), and (001) plateaus is to be found in polar plots of thermionic emission *versus* azimuth around the wire. Thermionic plateaus were discovered during the first sufficiently detailed preliminary thermionic measurements. These measurements were taken just before the conclusion of Table I, D, i.e., just prior to optical observation of the (112) and (001) plateaus. The final data polar plots of Fig. 8 show "flats" of thermionic emission in the (110), (112), and (001) directions; plateau widths can be had from Fig. 8 by adding 2.3°, the resolution of the emission measuring tube, to the widths of the emission flats. The values listed in Table II are taken from the 1810°K curve; they are seen to be in good agreement with those obtained from the photomicrographs. Studies of field emission from tungsten points of the order of 10^{-5} cm radius have shown emission flats in the same directions.[15–17]

At the same time that the photomicrographs were made, the diameter was measured by a simple optical wedge interferometer. The results are plotted as a function of azimuthal angle in Fig. 3. A definite upward departure from the average diameter is observed in the (001) direction and there may be a small upward departure in the (110) direction, but no minima are seen at the centers of these maxima. Note however that the deviation in diameter expected over an 11° plateau s 0.5 percent, or about two fringes of mercury green light, while that expected over a 7° plateau is one fringe. Moreover, the crystal section measured was located at the center of a 3.5-in. length of wire; although care was exercised in lowering the optical flat onto the wire, some slight twisting of the wire might have occurred if the flats came to rest in such a way as to impose a torque on the wire.

Just prior to removal from the emission measuring tube, the crystal was subjected to the temperature schedule of Table I, G, in an attempt to find some variation in plateau size as a function of temperature. Becker[16] has shown that on tungsten field emission points of about 3×10^{-5} cm radius, the steady state linear dimension of the (001) and (112) planes increases by a factor of almost two as the temperature is lowered from 2600° to 1200°K. He also found that the time necessary to reach a steady state increased as the temperature was lowered, a few seconds or less being required at 2600°K, while at 1200°K several minutes are needed. Since our tungsten wire is much larger than Becker's field emission point, the times used were much longer than his steady-state times. The 3030° and 1230°K heating periods were each preceded and followed by a rapid emission measurement, at 1560°K, of the widths of the 55° (112) and 90° (001) plateaus; the reading of the two widths required approximately 10 min. The three sets of width measurements agreed with one another to 0.1°, and indicate no experimentally observable change in plateau size under the stated limited temperature schedule.

III. DISCUSSION OF SURFACE STRUCTURE

The kind of surface structure observed on tungsten has been found by Nichols[18] on tantalum single crystals heated in vacuum, although no plateaus were observed on tantalum normal to the (112) directions. He has also found plateaus on molybdenum crystals. The formation of plateaus on tungsten, tantalum, and molybdenum must be due to one or more of three processes: (1) differential evaporation, (2) volume diffusion, and (3) surface diffusion. Herring[19] proposes that volume diffusion motivated by surface tension is mainly responsible for the plateau growth; he has developed, under certain reasonable assumptions, a theory that predicts remarkably well the size of tungsten and tantalum plateaus produced under different temperature schedules. Clearly, evaporation has no

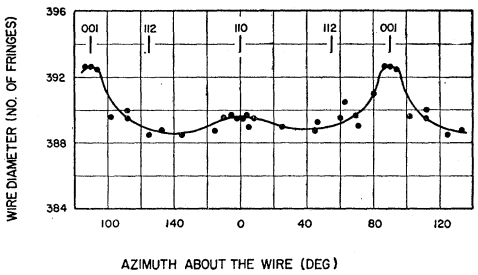

FIG. 3. Wire diameter as a function of angle around the wire. A simple wedge interferometer was used with mercury green light.

[15] E. W. Müller, Z. Physik **120**, 261, 270 (1943).
[16] J. A. Becker, Bell System Tech. J. **30**, 907 (1951); also by private communication.
[17] W. P. Dyke, Phys. Rev. **85**, 752 (1952).
[18] M. H. Nichols, following paper [Phys. Rev. **93**, 309 (1954)].
[19] Conyers Herring, *Structure and Properties of Solid Surfaces*, (University of Chicago Press, Chicago, 1953).

role in forming the structure on the 1980°K wire, although it must certainly be taken into account in a complete explanation of high-temperature structure. Herring[19] has pointed out that there is evidence that differential evaporation should tend to reduce rather than to enlarge the plateaus observed. He has also noted that at lower temperatures surface migration may be expected to become relatively more important, due to its lower activation energy.

Johnson[6] found no structure on single-crystal tungsten helices given ac heat treatment in vacuum sufficient to evaporate 17 percent of the wire diameter; from the known resolution of his observations, he concluded that there was no structure greater than a few thousand atom diameters in size on the crystals he studied. The structures observed here could just be resolved with optimum lighting. Although the plateaus are 10^{-3} cm wide, the structures are probably not much more than 5×10^{-5} cm in size and no larger than the upper bound set by Johnson. Thus it is possible that the plateaus on the helices were too small to be seen, particularly if Johnson did not use grazing incident illumination. However, Herring[19] suggests that the interchange of material between the surface of an *ideal* crystal facet and the region immediately below it may be so difficult as to inhibit the growth of such ideal facets. He points out that on Johnson's helices, facets would undoubtedly start as small elliptical spots of ideal orientation. Plateaus on long straight wires, on the other hand, are probably not exact (*hhk*) planes but vicinal planes, crossed by widely spaced transverse steps that would catalyze growth and dissolution. The shingle structure always found on long-wire plateaus is direct evidence of such transverse steps. Although Johnson found no plateau structure on vacuum-heated wires, he did report that flat surfaces appeared to develop in the (001) and (110) directions of crystals heated in lamp gas (86 percent argon plus 14 percent nitrogen) or in pure argon. He found that the (001) facets were larger than the (110) facets, whereas the reverse was observed in the present investigation. Evaporation is compensated for by condensation and produces no net material transport on a crystal in equilibrium with its vapor, as is approximately the case for a wire heated in a gas. On the other hand, the vacuum heated wire is subject to differential evaporation which could account for a (001) plateau of reduced width. Both the residual polishing marks and the maximum of diameter in the (001) direction can also be explained by differential evaporation. Using this hypothesis and the diameter plot of Fig. 3, Herring[20] has calculated an evaporation coefficient α_{001} of $\frac{1}{3}$ or $\frac{1}{2}$ or so. Using an analysis similar to that of reference 19, he has then shown that the (001) plateau width would be reduced to $\frac{2}{3}$ or $\frac{3}{4}$ of the value calculated[19] without differential evaporation, a result consistent with the observed plateau width.

The absence of a pronounced diameter maximum in the (110) direction must mean that there was almost no differential evaporation there. Herring has suggested two possible explanations.[20] First, the wire axis could be inclined to the (110) direction in such a way as to introduce steps close together on the (110) plateau but far apart on the (001). Second, the distance an atom can migrate before re-evaporation on the (001) plane may be substantially less than on the (110). In either case the evaporation coefficient α_{001} would be lower than α_{110}. This can be understood most easily by recalling that the principle of detailed balance requires the identity of the evaporation coefficient and the "sticking coefficient" for atoms impinging upon the surface from a vapor phase in equilibrium with the metal. An atom striking a plane surface from the vapor phase will be less likely to be incorporated into that surface if its chance to migrate to a step before being re-evaporated is small. This will occur if the steps are far apart or if distance migrated before re-evaporation is short; in either case α will be reduced.[21] Now from the last column of Table II it is seen that the wire axis lies very nearly in the 55° (112) plateau, since no shingling could be resolved on either the 55° or 235° plateaus. Then if the wire consists of one crystal and is truly cylindrical, the wire axis must make only a slightly larger angle with the 0° (110) plateau than with the 90° (001), so that steps on the (110) plateau should be spaced only slightly closer together than those on the (001) plateau. Close examination of the original photographs also shows (110) shingling only slightly more closely spaced than (001) shingling. Therefore, it seems that the second explanation is more plausible.

It is interesting to compare the rates of plateau growth with those obtained by Becker[16] for tungsten field emission points. Herring[22] has shown that under certain restrictions one can relate the times necessary to reach an equilibrium structure in two similar situations to the scale factor r of the two configurations. He has shown that if the mechanism is surface migration, the ratio of times to reach equilibrium will be r^4; if the mechanism is volume diffusion, the ratio will be r^3. Using these ratios and Becker's results, Herring[20] has calculated that it should take of the order of 5×10^5 days at 2400°K for sizeable plateaus to develop on 0.005-in. tungsten wires if the mechanism is surface diffusion. If the mechanism is volume diffusion, the time is reduced to about 3×10^3 days. Actually, plateaus are observed after only a few hours. Perhaps this discrepancy may also be due to inhibited plateau growth resulting from difficulty in interchange of material between the ideal crystal plane and the crystal bulk below that surface. As in the case of Johnson's

[20] Conyers Herring (private communication).

[21] See Appendix III of reference 10 for a discussion of smoothing by evaporation and related effects.

[22] Conyers Herring, J. Appl. Phys. **21**, 301 (1950).

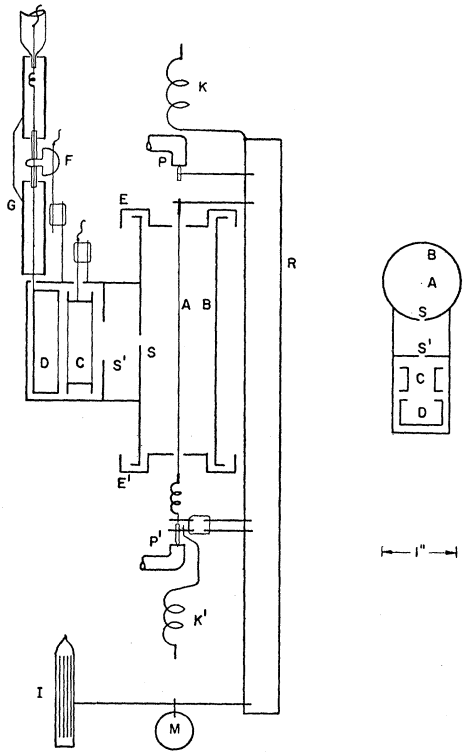

FIG. 4. Cross section and top view of tube used to measure the thermionic constants for different crystal directions. The crystal wire A is mounted in the rotor R so that it can be rotated in front of the slit S cut in the cylindrical anode B.

helices, Becker's field emission points must have facets starting in ideal orientation and hence would be subject to such inhibition, whereas the difficulty of interchange would not exist for the wires.

If the size of plateaus to be found on wires does vary with temperature in the range covered, the times used were not long enough to permit detection of such change. Of course, it is not likely that the wires ever reached an equilibrium structure, the rate of diffusion at low temperatures being too low, and evaporation disturbing any high-temperature equilibrium. The use of wires of smaller radius would be favorable for observations in shorter times.

IV. EQUIPMENT FOR THE THERMIONIC MEASUREMENTS

The tube used to make the quantitative thermionic measurements was originally designed and constructed by R. B. Nelson; it was first used to study crystallographic dependence of thermionic emission from tungsten single crystals by Nichols,[9] who rebuilt it to incorporate certain refinements. The tube was again rebuilt, with further modifications for the present measurements. Figure 4 is a schematic diagram of the metal parts of the tube as modified; the principal change from the tube as described in reference 9 is the addition of end guards E and E'. The slit S, 0.514×3.40 mm, is 3.1 times as small in area as that used by Nichols, giving an azimuthal resolution of 2.3° as compared with his resolution of 2.9°. The collimating slit S', 1.90×12.7 mm, does not serve to limit the beam.

The tube was pumped, outgassed, and sealed off by methods already described.[23] It is of interest that gas was released when the rotor R was first moved; care was taken to eliminate this gas before seal-off. A tantalum film getter along with a continuously operating Bayard-Alpert ion gauge[24,25] served to maintain a total pressure of about 1.5×10^{-9} mm of Hg for the entire period during which final measurements were made. "Emission decay" tests of 7 and 27 days duration at the outset and conclusion, respectively, of the final thermionic measurements showed no detectable change in emission in the (112) direction as measured at 1585°K. This indicates that the partial pressure of active gases, such as oxygen, was much lower than the total pressure, which probably consisted almost entirely of helium diffused through the glass.[26–28]

The Forsythe and Watson[29] temperature scale was used to determine the temperature of the middle section of the filament A. The 400-cycle alternating current used to heat the filament[30] was controlled by a thermionic regulator of the type first used by Ridenour and Lampson.[31] The rms value of the current was measured to better than 0.2 percent by comparison with a direct current producing the same heating effect in a 0.003-in. tungsten wire sealed in a tube containing hydrogen under a few mm of pressure. A Leed's and Northrup type-K potentiometer was used to measure thermal emf's and, with a standard 0.1-ohm resistor, the direct current. The best value of the wire diameter was obtained by use of an optical wedge interferometer; for the final thermionic data the average value from Fig. 3 is subject to a 0.2 percent correction due to evaporation[13] resulting from the heat treatment of Table I, G. The uncertainty in temperature due to 0.2 percent precision in diameter measurement is 3°K; that due to 0.2 percent precision in the current measurement is 2°K. Conduction cooling due to the finite length of the filament was observed in all Richardson plots for temperatures below about 1350°K, in good agreement with calculations based on tables given by Langmuir, MacLane, and Blodgett.[32]

Collector currents were measured by an Applied

[23] W. B. Nottingham, J. Appl. Phys. **8**, 762 (1937).
[24] R. T. Bayard and D. Alpert, Rev. Sci. Instr. **21**, 571 (1950).
[25] S. Wagener, Proc. Inst. Elec. Engrs. (London) **99**, Part III, 135 (1952).
[26] W. D. Urry, J. Am. Chem. Soc. **54**, 3887 (1932).
[27] W. H. Keesom, *Helium* (Elsevier, Amsterdam, 1942).
[28] D. Alpert, Phys. Rev. **89**, 902 (1953).
[29] W. E. Forsythe and E. M. Watson, J. Opt. Soc. Am. **24**, 114 (1934).
[30] In order to avoid the dc etch, as discussed in Sec. I, ac exclusively was used to heat the filament. Peak to peak temperature fluctuation at 800 cycles amounted to less than 1.5°K at 2000°K.
[31] L. N. Ridenour and C. W. Lampson, Rev. Sci. Instr. **8**, 162 (1937).
[32] Langmuir, MacLane, Blodgett, Phys. Rev. **35**, 478 (1930).

Physics Corporation vibrating reed electrometer[33] with one precision wire-wound and six Victoreen resistors. The anode voltage was supplied by a well-filtered full-wave rectifier circuit, *VR*-tube regulation being used for Richardson plots. Anode voltage was measured with the type-*K* potentiometer. All other electrode potentials were battery supplied.

Preliminary to actual use of the tube and before the end guards *EE'* were added, a complete set of operating characteristics was obtained to evaluate the effectiveness of, and correct operating point for, each of the auxiliary electrodes. Two forms of anomalous behavior, not previously reported by Nichols in his earlier work with the same tube, were discovered by their influence on the form of the operating characteristics. These spurious effects were more noticeable in the present investigation because (a) the slit *S* was reduced in cross section by a factor of three, and (b) operating characteristics were taken with the crystal oriented to measure a minimum of thermionic current. The orientation used by Nichols is not known, but judging from the nature of his characteristics and the order of magnitude of his collected currents,[9,34] it was probably not a direction of minimum emission.

Evidence of the first anomalous effect was found in the operating characteristic of the guard ring G. The proper guard ring potential required to shield the collector lead from stray electrons escaping from the open end of anode *B* (without end guards) was determined by plotting the collector current I_c *vs* the guard ring potential E_g with respect to the anode *B*. The collector was held at anode potential. Plots for crystal directions other than the minimum (110) were well-behaved and similar to that obtained by Nichols.[34] The plot taken with emission from the (110) direction (Fig. 5a) has two distinguishing features in addition to the expected peak in the negative vicinity of zero E_g. First, the current collected in the most negative guard ring region, although independent of E_g, has a much greater dependence on anode-cathode voltage E_p than does the current collected in the positive guard ring region. Secondly, there is an almost linear dependence of I_c on E_g for positive E_g. The first feature appears to be due to photoelectric emission from the guard ring, produced by x-rays of 1 to 3 kv from anode *B*, and collected by the collector lead due to the favorable field between it and the guard ring. The reverse phenomenon, photoelectric emission from the collector lead when E_g is positive, is not so pronounced due to the much smaller surface area of the collector lead. One cannot account satisfactorily for this first feature of Fig. 5a by mechanism (photoelectric effect, stray electron currents, field emission, ion currents) other than x-ray photoelectric emission. The second feature of Fig. 5a, the linear decrease of I_c with increasing E_g, appears to be due to electron emission from the glass surface of the insulator that supports the collector, particularly from the Pyrex wetting glass which provides a thin covering for the collector lead over several millimeters of its length. This emission is most likely secondary emission arising from bombardment of the glass by stray primary electrons, although there may also be some photoelectric emission produced by x-rays. Since the nearest electrode to this glass is the guard ring itself, the emission serves to charge the surface of the glass to the potential of the guard ring. From the slope of the curves of Fig. 5a, the resistance of the leak is 5×10^{13} ohms, a value consistent with the resistivity of Pyrex, 10^{14} ohm cm, and the dimensions of the wetting glass. The anode potential dependence of I_c observed for a constant positive E_g is very nearly in agreement with the Schottky mirror image theory, as might be expected if the Schottky dependent emission has a small constant superposed leakage current. Further evidence of dielectric charging is given by long times required for reaching equilibrium after changing conditions in the measuring tube, especially if a change in E_g is involved. Nichols reported a similar time effect for measurements in the (110) direction.[34] A volt-ampere characteristic for the guard ring also was consistent with the above explanations of both features of the first anomalous effect.

The choice of a completely satisfactory operating point on the curves of Fig. 5a is of course impossible. However, since the slope on the E_g positive side is significant only for low temperatures *and* in the (110)

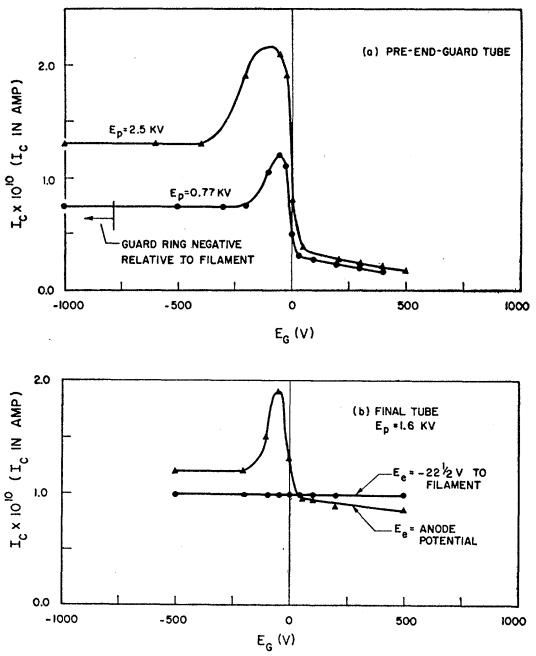

FIG. 5. Guard-ring characteristics before and after elimination of first anomalous effect. Data taken in (110) direction at 1690°K.

[33] Palevsky, Swank, and Grenchik, Rev. Sci. Instr. **18**, 298 (1947).

[34] M. H. Nichols, Massachusetts Institute of Technology, Ph.D. thesis, 1939 (unpublished).

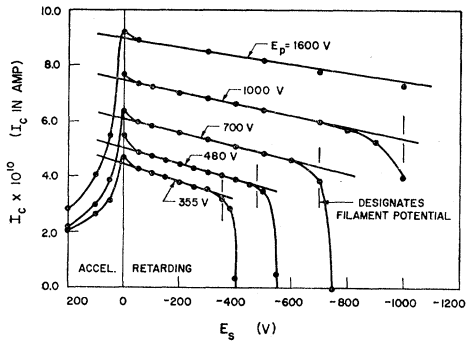

FIG. 6. Suppressor characteristics for final tube showing second anomalous effect. Data taken in (110) direction at 1805°K.

direction, and since the x-ray photoelectric current is large only for negative E_g, a value of 180 v positive was chosen for the unmodified tube as used to obtain the "pre-end-guard" data. Before taking the final data, the end guards EE' were installed as shown on Fig. 4. Their presence and operation at 22.5 v negative with respect to the filament served to eliminate both radiation and stray electrons from the vicinity of the guard ring, as can be seen from the guard-ring characteristic of Fig. 5b. Their operation at anode potential, however, does not eliminate the glass charging effect, indicating that it is at least partly due to stray electrons from the end of the anode. No distortion was introduced in the field at the slit by the presence of the end guards, as evidenced by constant collector current for a maximum emission direction when the end guards were varied separately or simultaneously from anode to filament potential.

The second anomalous effect was revealed by its influence on the operating characteristic of the secondary suppressor C. This effect was observed even after installation of the end guards. For all directions of emission except those near the (110) minima there was no observable variation of collector current I_c *vs* suppressor voltage E_s with respect to the anode, provided that E_s was sufficiently negative to repel and return slow secondaries generated at the slits and at the collector D, the collector being at anode potential. Nichols'[34] suppressor characteristics were also of this form. On the other hand, suppressor characteristics for the (110) direction are given in Fig. 6. There is considerable evidence that this behavior is due to collection through the slit system of secondary electrons emitted at the anode B, secondaries coming from anode regions upon which the impinging emission density is much greater than the emission density in the direction of the slits. Although the angular resolution of slit S to emission from the wire is only 2.3°, the much larger slit S' is not designed to collimate the beam, and electrons proceeding at angles up to 6° or 7° with the radial direction can penetrate the slits to reach the collector D. Moreover, the vertical resolution is very poor indeed, due to the length of S and emphasized by the excessive length of S'. A typical electron path is shown in Fig. 7. The trajectory was calculated by a graphical stream plotting method for an electron leaving the anode at 5° from the normal, with one-half of the primary electron energy. This electron originated at 120° in azimuth, measured from the slit. The curves of Fig. 6 are essentially integrated energy distribution curves of the current through the slits. The form of the curves indicates an energy distribution similar to that known for secondary emission.[35–37] There is a low-energy peak, an almost constant distribution over medium energies, and a large full-energy peak. Indeed, if it were not for the full-energy component of the secondary emission it would be a relatively simple matter to use the suppressor characteristic to subtract out all but the full-energy thermionic emission. The curves of Fig. 6 indicate that the spurious effect is at least as pronounced at low anode voltages as at higher ones. Although not too much is known about primary energy dependence of secondary emission components, the total secondary emission ratio is known to have a maximum at about 600 v for tantalum.[38] Suppressor curves for various temperatures show the effect to be relatively larger at lower temperatures. This would be expected since the surfaces producing the abundant primary emission responsible for secondary emission are of lower work function than the (110) surface. Elimination of the second anomalous effect was not undertaken. The technique of correction used to obtain (110) data will be described in Sec. V. For directions other than the (110), the suppressor electrode was operated at −540 v with respect to the anode, except for retarding potential plots.

As long as the collector D was positive with respect both to the filament and to the suppressor, there was no dependence of collector current upon collector voltage. Except for retarding potential plots the collector was operated at anode potential.

V. THERMIONIC DATA FROM SINGLE CRYSTAL OF TUNGSTEN

Two complete sets of thermionic data were obtained: (a) the pre-end-guard data, subject to both anomalous

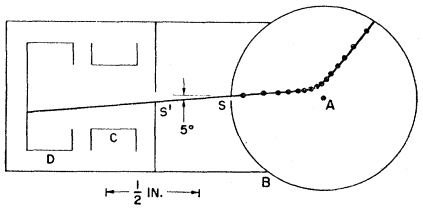

FIG. 7. Graphically computed path of a secondary electron emitted from anode so as to enter slits SS' to be collected at D. The electron is emitted with one-half primary energy at 5° to the radial direction.

[35] K. G. McKay, *Advances in Electronics* (Academic Press, Inc., New York, 1948), Vol. 1.
[36] Erick Rudberg, Phys. Rev. **50**, 138 (1936).
[37] L. J. Haworth, Phys. Rev. **48**, 88 (1935).
[38] L. R. Koller, Gen. Elec. Rev. **51**, 33, 50 (1948).

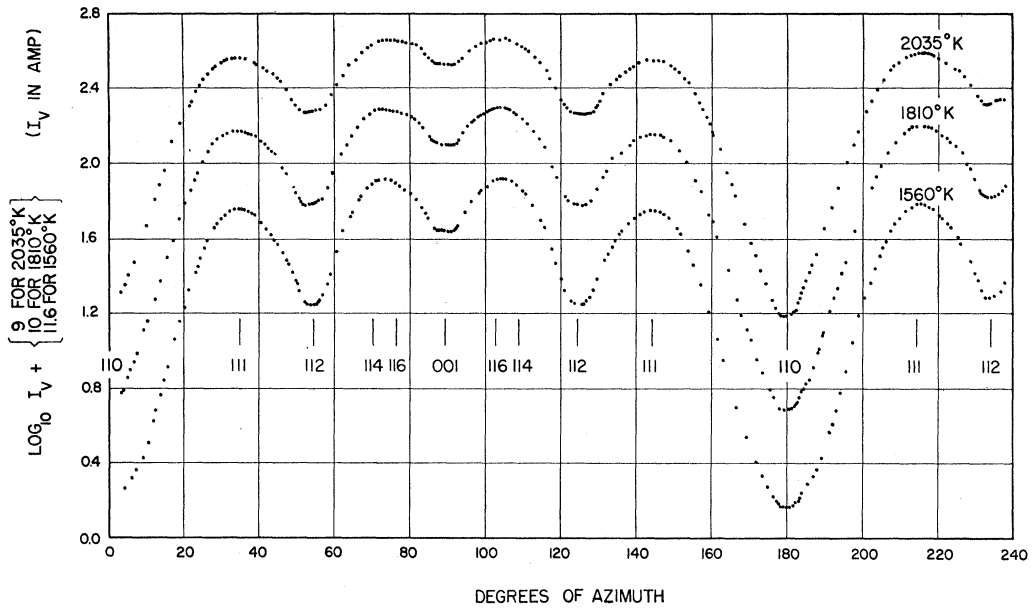

FIG. 8. Emission *vs* azimuth; $E_p=1600$ v, corresponding to surface gradient of 5.5×10^4 v/cm.

effects, and (b) the final data, with end guards installed to eliminate the first anomalous effect. The pre-end-guard data were taken with the tube basically as used by Nichols; the results show good agreement with those he obtained. The first anomalous effect is important only in directions of low emission, as will be seen from Richardson plot comparisons. The second anomalous effect, not eliminated in either set, seriously affects the measurements only in the (110) direction, where the data have been partially corrected, as will be described. At the conclusion of the final run the wire was flashed for one min at 3030°K to check reproducibility of the data. For no crystal direction did emission after the flash differ by more than 5 percent from the pre-flash value.

In Fig. 8, polar plots of emission *vs* azimuth about the wire were obtained by rotating the crystal wire before the slit system. Assignment of crystal directions is in agreement with previous work.[4,9] The distinguishing feature of the polar plots is the appearance of definite "flats" in the directions of minimum emission. This corroborates the visual observation of plateaus on the wire, as discussed in Sec. II. Nichols' polar plots[9] did not show these flats. This can be due to: (1) an insufficient number of points in his curves together with slightly poorer resolution, or (2) a different heat treatment of his crystal. Although the heat treatment Nichols gave his crystal after repolishing and before taking thermionic data was sufficient to give reproducible results, it was quite mild compared to that given here. However, since plateaus have been optically observed on wires given only very mild heat treatment (see Sec. II), the more probable explanation is (1). The data of Fig. 8 were taken with the final tube; the emission flats were found on preliminary runs, but there had been heat treatment sufficient to produce 2.5 percent wire diameter reduction due to evaporation before the first sufficiently detailed run was made. It should be noted that currents smaller than that in the (112) direction are not reliable, owing to the second anomalous effect. For this reason, it is also not certain that the (110) plateau width derived from Fig. 8 is accurate.

Schottky plots of emission *vs* anode-filament potential E_p were taken at two temperatures for each direction corresponding to a maximum or minimum of emission. Illustrative final tube curves are shown in Fig. 9. The pre-end-guard data did not differ significantly from the final data except in the (110) direction, where the former were difficult to obtain due to glass charging effects. The slope S of the Schottky line (the coefficient of $E_p^{\frac{1}{2}}/T$) was used to reduce the high field emission to zero field conditions. Agreement of slopes for the two temperatures was within 5 percent. Average values are tabulated for each direction in Table III. The numerical values of slope are considered to be within experimental error of the mirror image theoretical value for a uniform surface, except in the (110) direction. The (110) data will be discussed separately below. Evidence is seen on the Schottky lines of the periodic Schottky deviation.[39–42] The upper voltage limit of 2800 v, imposed by the onset of field emission from tube parts, limited the voltage range of the tube to about one cycle of the deviation, making it difficult to choose a reference line for the fluctuation.

[39] R. L. E. Seifert and T. E. Phipps, Phys. Rev. **56**, 652 (1939).
[40] D. Turnbull and T. E. Phipps, Phys. Rev. **56**, 663 (1939).
[41] W. B. Nottingham, Phys. Rev. **57**, 935 (1940).
[42] Munick, LaBerge, and Coomes, Phys. Rev. **80**, 887 (1950).

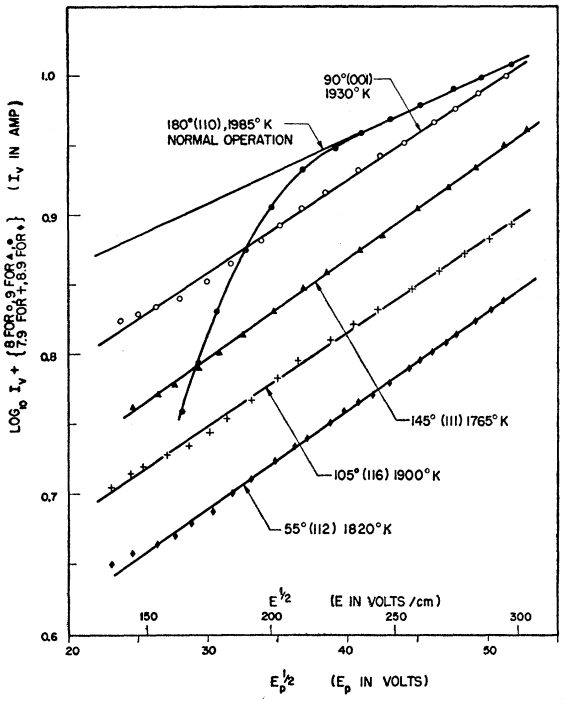

FIG. 9. Illustrative Schottky plots.

No attempt was made to study the periodic deviation due to the limitations of the tube. Directions other than the (110) show no deviation from the Schottky line, aside from the periodic deviation, for voltages higher than 750, corresponding to a gradient of 26 000 v/cm. A simple calculation shows that the upward deviation in the (112) and (001) directions at this point is clearly the result of failure of projection properties of the tube due to thermal velocities. Similar deviation occurs only at even lower potentials for the high-emission directions, as might be expected in view of the broad nature of the peaks of emission (Fig. 8). Patchiness, either small or large scale, can produce only downward deviation in the (112) and (001) directions.

Richardson plots of emission *vs* temperature were taken in each minimum and maximum emission direction. The apparent emission constants for uniform and for patchy surfaces are defined and discussed by Herring and Nichols.[10] The experimental constants will be doubly starred because there is insufficient evidence to show that the exposed surfaces are not patchy. Illustrative Richardson plots for the final and pre-end-guard tubes are given in Fig. 10. Complete results from both tubes appear in Table III, along with the values obtained by Nichols.[10] Difference between the final and the pre-end-guard data is a measure of the first anomalous effect. Except in the (110) direction the effect is seen to be small.[43] Data from high-emission surfaces were essentially unaffected while low-emission Richardson plots were reduced in φ^{**} and A^{**} by elimination of the effect. Pre-end-guard operation, with guard ring at +180 v, is subject to the reduced anomalous effect of x-ray photoelectric emission from the collector lead, which should produce just such an effect. The spurious photoelectric emission produces a relatively larger reduction in measured current at low temperatures, since the x-ray are generated by an average (relatively low work function) emission. The low-temperature droop in the (110) Richardson line is a consequence of collector insulator charging and leakage as discussed in Sec. IV. All other Richardson lines show downward departure for temperatures below about 1350°K. This is due to reduction in temperature by conduction to the ends of the wire (see Sec. IV). Slight systematic downward departure from a straight line is also observed for high temperatures. Careful check of the current measuring apparatus leaves uncertainty in the temperature scale as a possible source of this deviation.[44]

Data for the (110) direction, *taken in the same way as for other surfaces*, are in good agreement with those obtained by Nichols.[9] Both the final tube and the pre-end-guard tube gave Schottky plots with slightly lower than average slope and with definite departure from the Schottky line at about the same surface gradient as observed by Nichols. The final tube Schottky plot for the (110) direction is given along with valid plots for other directions in Fig. 9. The pre-end-guard thermionic constants obtained by normal operation of the tube (Tables III and IV) are in good agreement with Nichols' constants. It will be recalled that the crystal used was selected with the purpose of eliminating the shingle structure on the (110) surface. Although shingling was not in fact completely missing, the degree of shingling was greatly reduced from that encountered by Nichols. If the shingling were indicative

TABLE III. Thermionic constants for the different crystal directions. Both final and pre-end-guard values are tabulated. Nichols' results, reference 10, are given for comparison. The precision of φ^{**} is about 0.5 percent, that of A^{**} about 10 percent; S is the Schottky slope.

	Final			Pre-end-guard			Nichols	
Direction	φ^{**}	A^{**}	S	φ^{**}	A^{**}	S	φ^{**}	A^{**}
35° (111)	4.39	54	12.8	4.38	55	11.9		
145° (111)	4.37	47	12.8	4.36	49	12.0	4.39	35
215° (111)	4.38	54	12.3	4.39	65	10.6		
55° (112)	4.65	118	12.8	4.68	163	12.9		
125° (112)	4.64	110	13.2	4.68	150	12.5	4.69	125
235° (112)	4.65	133	11.5	4.66[a]	153[a]	10.8		
75° (116)	4.29	40	12.8	4.31	48	12.2	4.39	53
105° (116)	4.29	40	12.3	4.30	46	12.0		
90° (001)	4.52	105	12.7	4.52	119	12.4	4.56	117
180° (110)[b]	4.58[b]	8.0[b]	9.1[b]	4.66[b]	11.8[b]	10.4[b]	4.68[b]	15[b]
Theoretical			11.2			11.1		

[a] Unreliable data due to deterioration of vacuum over long interval between remainder of pre-end-guard tube data and this measurement.
[b] Anomalous behavior invalidates (110) data obtained under normal operating conditions. True (110) current smaller than these figures indicate.

[43] The location of the pre-end-guard Richardson lines *above* the final lines is probably due to error in pre-end-guard wire diameter, obtained by 0.61 percent correction for evaporation from final line value; see reference 14.

[44] Temperature dependence of work function can produce curvature of the Richardson line. It will be recalled, however, that a *linear* temperature dependence of φ for a *uniform* surface will produce no curvature. Although patchiness can produce curvature, it will always be concave upward.

of patchiness on the (110) surface and if that patchiness were responsible for departure from the Schottky line, one would expect higher φ^{**} and A^{**} from the present measurements, rather than the slightly lower pre-end-guard values obtained. When the first anomalous effect was eliminated in the final tube, the constants were affected in the same way as were those of other low-emission surfaces, but to a larger degree. The more important second anomalous effect, due to secondary emission, can be partially eliminated by using the suppressor C as a retarding barrier. By extrapolating suppressor characteristic curves (Fig. 6) to the filament potential one can eliminate all but full-energy electrons to the collector. The "extrapolated" Richardson plot obtained in this way (Fig. 11) has emission constants $\varphi^{**}=4.72$, $A^{**}=9.7$, which set a definite upper limit for the true (110) emission. An estimate of the value of the true (110) work function can be made under two assumptions: (a) that all of the secondary emission current has the same effective work function, and (b) that, as has already been found for the similar (112) and (001) surfaces, $A^{**}_{(110)}\approx 120$. Under assumption (a), the difference between the left and right extrapolations of the suppressor characteristic is taken as a measure of the secondary emission current, and an effective work function, 4.42 v, is obtained from a "Richardson plot" of this current (Fig. 11). Then by a method of successive approximations, just enough spurious current with this effective work function is subtracted to leave a Richardson plot with $A^{**}=120$. The apparent work function of the estimated (110) line so obtained is 5.26 v. The agreement between the spurious current effective work function, 4.42 v, and the average work function of doped polycrystalline tungsten,[3] 4.45 v, suggests that the secondary emission as obtained here is indeed dependent upon a high-field average over all of the crystal, supporting assumption (a). To illustrate the magnitude of concave upward curvature expected in the "extrapolated" Richardson plot,[10] straight 5.26 and 4.42 v Richardson lines were added to give a perfect match to the experimental curve at $10^4/T$ of 5.3 and 6.2. Points on this computed line are plotted as triangles in Fig. 11; it is seen that the curvature produces a negligible deviation from the straight line in the range of temperature for which data are available. Due to dependence of the secondary

TABLE IV. Summary of (110) data.

Description	φ^{**}	A^{**}
Nichols' values, reference 10	4.68	15
Pre-end-guard, normal operation	4.66	12
Final tube, normal operation	4.58	8.0
Final tube, extrapolated	4.72	9.7
Pure spurious current, effective slope	4.42	
Estimate by subtraction of spurious current to give $A^{**}=120$	5.26	120
Contact potential (implicitly assuming $A^{**}=118$)	5.21	118

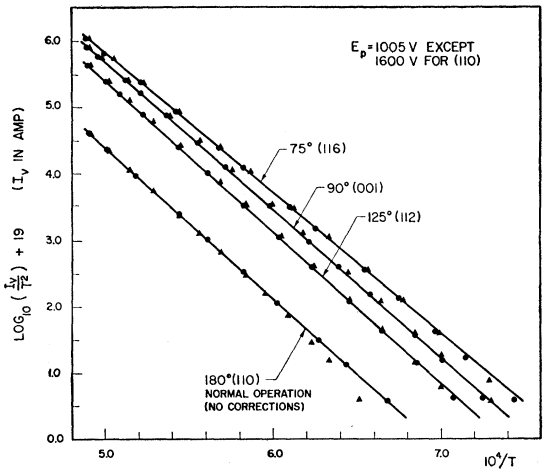

FIG. 10. Illustrative Richardson plots of pre-end-guard data ▲ and corresponding final tube data ●. The Richardson lines are drawn for the final data.

emission process on primary energy, no data significant in the usual sense could be obtained from a (110) Schottky plot by extrapolation procedures. The plot shared the rapid downward trend at low voltages which marked the original unextrapolated Schottky curves, but for higher voltages it became almost constant; 745 v was chosen as the optimum anode-filament potential difference consistent with satisfactory projection properties of the tube. Since no meaningful Schottky slope was available, the theoretical slope of 11.2 was used to correct the data to zero field values. A summary of various apparent thermionic constants for the (110) direction appears in Table IV.

Although the tube as described was not designed for measurements using retarding fields, operation with the collector within a few volts of the filament potential permitted the taking of retarding potential curves for the various crystal directions. The anode was held at 1005 v to maintain the projection properties of the tube. The maximum deviation from the mean filament potential due to ac drop amounted to 0.13 v. Although there was no completely satisfactory operating potential for the suppressor electrode C, the results to be reported were taken with the suppressor 3 v positive with respect to the filament, the value which gave maximum collected current. Data taken with the suppressor at collector potential or at 1.5 v negative with respect to the collector were essentially the same. Retarding potential curves for one each of the (111), (112), (116), (001) and (110) surfaces are given in Fig. 12. As expected, all curves, except the (110), merge for strongly retarding fields.[45] The slope for strongly retarding fields represents a temperature of 2090°K,

[45] The fact that the curves, other than the (110), do not coincide precisely for strongly retarding fields is probably due to slight differences in temperature among the runs. However, the short time stability of the filament current regulator did not permit significant temperature drift during one retarding run.

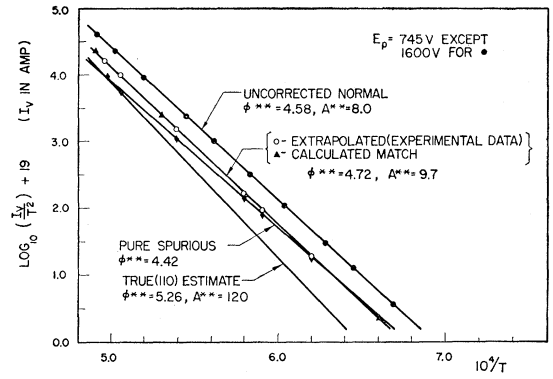

FIG. 11. Final tube Richardson plots for the (110) direction. Data plotted are: (1) uncorrected normal, taken as for other directions without correction for secondary emission effect; (2) extrapolated, giving a conservative upper limit for the "true" (110) current; (3) pure spurious, representative of the spurious secondary current alone; (4) estimate of the true (110) current.

whereas the value computed from the filament current and the Forsythe-Watson temperature scale is 1990°K. The saturation values have been designated somewhat arbitrarily, since the values indicated represent only about 55 percent of the current collected under normal accelerating conditions at the same temperature. However, the fraction collected is the same for each direction (except for the (110), where the fraction is 34 percent of the extrapolated Richardson current). The remainder of the slit current is divided between the suppressor C and the anode in the unfavorable electron optical configuration. That the (110) saturation value is low indicates more complete elimination of spurious secondary current under retarding conditions. Except for the (110) direction, no new information is to be had from contact potentials from pairs of retarding potential curves,[46] since the saturation current is equivalent to a Richardson line point, and the curves have the same tangent for strongly retarding fields. But in view of the reduced (110) saturation value, it is interesting to obtain a contact potential for that direction. The value obtained with the 55° (112) curve, taking the difference in abscissas of points A and B of Fig. 12, is 0.64 v, giving $\varphi_{(110)}{}^{**}=5.29$ v. Point B is taken on the common tangent since the (110) curve must merge with that curve for sufficiently retarded conditions. This φ^{**} value[47] contains the implicit assumption that $A_{(110)}{}^{**}=A_{(112)}{}^{**}$. Since $A_{(112)}{}^{**}=118$, this is equivalent to assumption (a) of the previous paragraph. However, the comparison does not involve a subtraction of spurious current; thus it gives a more reliable upper limit for the true (110) emission at this temperature. The shape of the retarding potential curves can sometimes give information about the patch nature of the emitter.[48] Patchiness produces a breaking away from the corner of a retarding potential curve. Unfortunately, the departure from an ideal plane parallel configuration also causes a rounding off of the corner, making the observation of patch effects more difficult. From the shape of the curves of Fig. 12, it is clear that the ac filament drop does not make a large contribution to the rounding. Although the curves are all of very nearly the same shape, that for 55° (112) shows the least rounding at the breakpoint. In Fig. 13 the 75° (116) curve is compared with the 55° (112) curve by matching saturation currents and currents for most retarded conditions. Excluding the (110) direction which will be discussed in the next section, the comparison is typical, the poorest match occurring between the 235° and 55° (112) directions. To give some idea as to what sort of rounding off patchiness might produce, two-patch curves were computed to match the 75° (116) emission. The 55° (112) curve was taken as characteristic of a uniform surface and proper proportions of current from two such curves, displaced in abscissas, were added to obtain a retarding potential curve for the two-patch surface. Using Fig. 12 of reference 10, patches with $A=120$ and no work function temperature dependence were chosen to give the

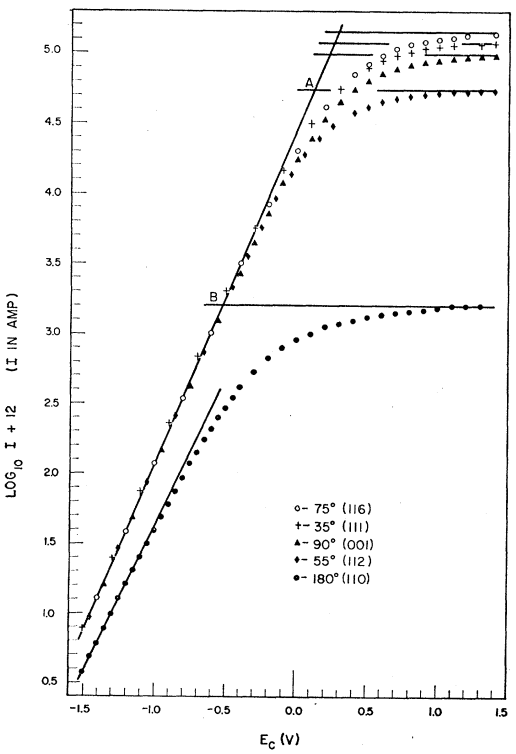

FIG. 12. Retarding potential curves for representative directions (final tube data); $E_p=1005$ v.

[46] As pointed out by Herring in private communication. The view taken in the U. S. Office of Naval Research Report N6-onr-24433 (unpublished) on this matter is erroneous.

[47] One notes that the same values are obtained by arbitrarily taking $A_{(110)}{}^{**}=118$ and choosing $\varphi_{(110)}{}^{**}$ so that Richardson's equation will give the saturation (110) current of Fig. 12.

[48] See reference 10 for a discussion of retarding potential plots for patchy emitters.

experimentally observed emission constants $\varphi^{**}=4.30$, $A^{**}=40$. From reference 10 it is seen that a $\delta\varphi \geqslant 0.4$ v is required to give $A^{**}=40$. For $\delta\varphi=0.4$, 10 percent of the surface must have $\varphi_1=4.20$ and the remainder $\varphi_2=4.61$. For $\delta\varphi=1.0$, one may have 33 percent $\varphi_1=4.30$ and the remainder $\varphi_2=5.30$.[49] Retarding curves for these two composite surfaces are plotted along with the experimental curves in Fig. 13. The two-patch curves do show a larger falling-off in the vicinity of the breakpoint than does the experimental curve. However, it is not certain that a larger number of patches might not give smaller departure in form from the uniform surface retarding potential curve.[50]

VI. DISCUSSION OF EMISSION MEASUREMENTS

Since the first anomalous effect produced only small changes in the thermionic constants, and since the second effect was negligible (except in the (110) direction), it is reasonable to compare data (Table III) with those obtained by Nichols.[9] In general, the precision limits overlap. However, $\varphi_{(116)}{}^{**}$ is 0.09 v lower than Nichols' value. It is possible that the difference is due to different wire heat treatments before measurements were made. Although the treatment Nichols gave his crystal after repolishing and before taking thermionic data was sufficient to give reproducible results, it was quite mild compared to that given here. It is likely that the treatment of Table I, CDEF produced material transport responsible for the difference in $\varphi_{(116)}{}^{**}$. (111) constants are in good agreement, showing that the effect, if any, of the dc etch on Nichols' crystal apparently did not extend to the (111) direction.

It has been shown that (110) data taken in the same way as for other surfaces are seriously affected by the second anomalous effect even after elimination of the first anomalous effect. Indeed, both the break in the (110) Schottky plot and the very low value of $A_{(110)}{}^{**}$ reported by Nichols and observed here are probably entirely due to this secondary emission effect, rather than to patchiness on the (110) surface. The shape of the (110) retarding potential curve of Fig. 12 also is undoubtedly influenced by remaining spurious current. However, when the retarding barrier at the collector becomes higher than the emitter surface barrier of any patch, one would expect the true (110) current to merge into the common line, as was the case for all other surfaces. The fact that it lies *below* that line for the most retarded potentials used clearly indicates a deficiency rather than a surplus of current. This can be explained by (1) the presence of a high work function patch on the (110) surface, (2) a large reflection coefficient for the (110) surface, or possibly (3) a failure of projection properties of the tube in the (110) direction. The (110) curve has not yet joined the common tangent at -1.5 v in Fig. 12. The (112) curve joins the tangent at about -0.4 v. If (1) is the explanation, this would indicate the existence of a patch on the (110) surface more than 1.1 v higher than $\varphi_{(112)}{}^{**}$, at least 5.7 v and likely as high as 6.0 v. Since a Schottky plot could not be obtained for the (110) direction, (2) and (3) cannot be ruled out. However, tangential patch fields near the (110) direction would have to be much higher than those near the (112) direction for failure of projection properties since (112) Schottky plots showed satisfactory projection properties until thermal velocities became important. Assuming satisfactory projection in the (110) direction, one can say from the saturation value of the (110) retarding potential plot that the (110) emission at 1990°K is no larger than would be given by $\varphi^{**}=5.29$, $A^{**}=118$. There is no justification for that arbitrary choice of A^{**} except the similarity among the (110), (112), and (001) surfaces. All of them have plateaus with shingling, and each of the latter two has A^{**} near 120. From the extrapolated Richardson plot one can say that the (110) emission at any temperature within the range covered is no larger than that given by $\varphi^{**}=4.72$, $A^{**}=9.7$, although this certainly includes some of the spurious current.‡

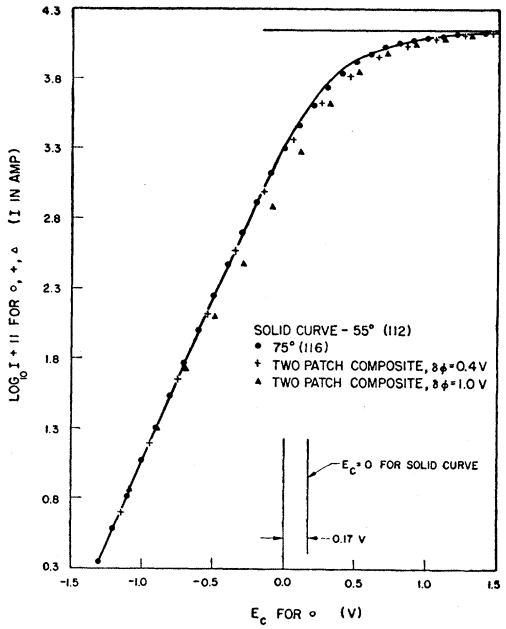

FIG. 13. Comparison of 75° (116) and 55° (112) retarding potential curve shapes. Calculated two-patch curves matching the 75° (116) emission are also plotted.

[49] Although Fig. 12 of reference 10 shows two ways of obtaining the desired φ^{**} and A^{**} with $\delta\varphi=1.0$ v, the one with the higher percentage of low work function patch has been chosen. This avoids excessive curvature of the Richardson plot for the two-patch surface.

[50] Two-patch curves were also computed to match the 35° (111) emission. The results were very similar to those for the 75° (116).

‡ *Note added in proof.*—Drechsler and Müller, Z. Physik **134**, 208 (1953), M. Wilkinson, J. Appl. Phys. **24**, 1203 (1953), and Dyke, Trolan, Dolan, and Grundhauser, J. Appl. Phys. **25**, 106 (1954), have recently reported field emission $\varphi_{(110)}$ values of 5.70, about 4.7, and about 5.2 v, respectively. Drechsler and Müller's value is derived from measurements first reported in reference 15;

Values of A^{**} not equal to 120 can be explained by one or more of the following effects: (a) patch effects, (b) temperature dependence of work function, and (c) reflection effects. Theoretically and on the basis of studies of periodic Schottky deviations there is reason to believe that under high field conditions reflection effects are small for tungsten.[10] Although periodic Schottky deviations for the individual crystal directions were not studied in detail, the curves of Fig. 9 indicate that the surfaces with low A^{**}, notably the (116) and (111), do not show deviations appreciably different in magnitude from those for the other surfaces. If one knew the patch nature of the surface of the single tungsten crystal, it might be possible to distinguish between (a) and (b) as responsible for the experimental values of A^{**}. Herring and Nichols[10] have already suggested that the values near 120 for the (112) and (001) directions are consistent with uniform surfaces having no net work function temperature derivative. However, there is insufficient evidence to show conclusively that the (111) and (116) surfaces are not patchy. As discussed in Sec. III, a hill-and-valley surface is a possible quasi-equilibrium structure on a relatively large crystal. There is, on the other hand, no evidence other than the variation in A^{**} that the (111) and (116) surfaces *are* patchy. Microscopic examination of the crystal surface, capable of resolution to about 1μ, showed no structure except the plateau and shingle structure already discussed. The plateaus appear to be associated with simple facets exposed on the single crystal; the fact that the range in degree of shingling encountered had no effect on the emission would indicate that such structure does not represent a significant patchiness (at least in the (112) and (001) directions). Tangential fields due to patches of 1μ linear dimension and 0.5 v work function difference would be of the order of 0.5×10^4 v/cm and should easily affect the slope of a Schottky line at 2.0×10^4 v/cm, the lower limit of the Schottky plots of Fig. 9. The experimental Schottky lines were straight and had essentially theoretical slope for fields up to the limiting value of 1.0×10^5 v/cm. If the region plotted lies entirely below the anomalous Schottky region due to a fine scale patchiness (case 2 of reference 10), the patch fields would have to be of the order of 10^6 v/cm. Again assuming a 0.5 v work function difference, this would require a patch dimension of the order of 50A, only one order larger than the lattice spacing. Finally, the retarding potential plots (excluding the (110) plot) showed no significant rounding of the corner due to a patchy emitter. However, the calculated two-patch curves show that for the unfavorable electrode configuration used, the shape of the retarding potential curve is not a sensitive test for patchiness. Thus it appears that visual observation and straight Schottky lines of theoretical slope rule out large and medium scale patchiness, leaving a small scale effect possible.

Especial gratitude is due to M. H. Nichols, who suggested the problem, for his continued interest and inspiration, for stimulating discussions, and for his many suggestions. I am indebted to Conyers Herring for much of the interpretation of the surface structure observations and for reading the manuscript. I am also grateful to the Standard Oil Company of California for the Standard Oil Fellowship, during the tenure of which part of this work was done.

---

they measured the (110) current through a small anode aperture. The other two values were obtained by phosphor brightness measurements. Dyke *et al.* took special precautions to minimize light scattering into the faint (110) areas.

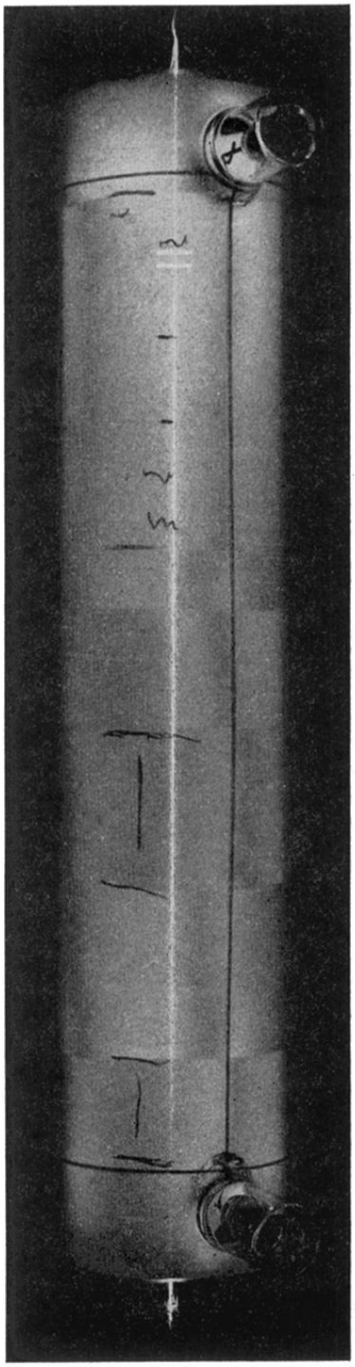

FIG. 1. Projection tube pattern of wire containing single crystal section used for quantitative thermionic measurements. The white marks set off the single crystal section; the dark marks are crayon lines on the tube for identification purposes.

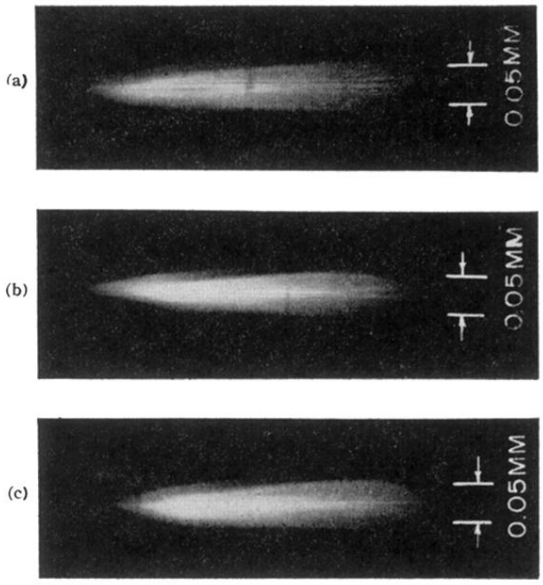

FIG. 2. Photomicrographs of single crystal showing plateau structure. (a) 180° (110) plateau; (b) 235° (112) plateau; (c) 90° (001) plateau.